

**DEVELOPMENT OF A MODEL FOR RAMPING
IN A STORAGE RING***

Kevin J. Cassidy

Tektronix Federal Systems, Inc., Irvine CA 92714

Sam Howry

Stanford Linear Accelerator Center, Stanford, CA 94309

ABSTRACT

This paper describes the process of ramping in a storage ring such as the SPEAR Synchrotron Radiation Ring at SLAC/SSRL. A definition of ramping is presented first. Then an "ideal" ramp that includes the necessary calibrations is presented. This is refined to account for nonzero response times that may occur in an "actual" ramp. Parameters are identified which cause the actual model to deviate from the ideal. A process to estimate these parameters is described that depends on rapid measurement of the ring's tunes. Finally, the paper describes a digital signal processor (DSP) that was used at SPEAR to measure the tunes during a ramp.

*Presented at the 1991 Accelerator Instrumentation Workshop,
Newport News, VA, October 28-31, 1991.*

* Work supported by Department of Energy contract DE-AC02-76SF00515

INTRODUCTION

This paper describes the process used to ramp electrons in the SPEAR Synchrotron Radiation Ring. Although ramping in a storage ring is certainly not new,¹ it is detailed here, so that future ring designers can contemplate the problem. The ramping software is part of the PEP/SPEAR control system.² The ramping model is defined first; then values of certain control parameters are refined with the help of a digital signal processor (DSP) that can measure actual ramp tunes online.

1. DEFINITION OF THE RAMP

Lattice designs for storage rings³ work with a set of strengths \mathbf{S} of controllable elements (such as quadrupoles, sextupoles, rf voltages) and with a set T of Twiss functions, which describe the focusing characteristics of the beam at any geometric position s along the beamline. In a storage ring, Twiss functions $\beta(s)$, $\alpha(s)$, $\eta(s)$, and $\eta'(s)$ are periodic (period = 1 ring revolution). The monotonic tune advance function $\Delta\nu(s, s + \Delta s)$ increases by a fixed constant ν , called the tune, whenever $\Delta s = 1$ period. There are horizontal, vertical, and longitudinal components of the Twiss functions, although in most systems some components are identically zero. The fractional part of the three tune constants: ν_x , ν_y , and ν_s can be directly measured when there is a stored beam in the ring.

Typically, the output from a lattice design program is a set of strengths \mathbf{S} that produces a specified set of Twiss functions T . Often it is desirable to inject particles into a ring configured at energy E_0 and strengths \mathbf{S}_0 (corresponding to Twiss functions T_0) and then to slowly change the ring to a final configuration of energy E_{final} and strengths S_{final} , while keeping the stored particles in the ring. This operation is called ramping. In a pure energy ramp, $S_0 = S_{final}$; only the energy is changed. Ramping allows a storage ring to operate with a relatively inexpensive, lower energy injector.

2. THE “IDEAL” RAMP MODEL

The energy of a storage ring is determined by $\int Bdl$ of all of its dipole (bending) magnets. The dipoles are often all on one series circuit. This circuit may also supply part of the current that determines some of the strengths, with the exact values of these strengths being controlled by individual shunt or booster supplies.

The ramping model must convert energy and strengths (E, \mathbf{S}) into integers for actual power supply controllers, and vice versa. This is the one to one, invertible mapping:

$$\Phi(E, \mathbf{S}) \Rightarrow \text{DAC integers} \quad (1)$$

for the dipole controller(s) and for controllers of all of the focusing elements (see figure 1).

The map is roughly linear for most systems, but it is by no means linear enough for ramping. Before the ramp begins, DAC setpoints are calculated from the map and stored in a table for each independent control and for each ramp step. The number N of ramp steps and the number Δt of milliseconds between ramp steps are parameters that can be changed by the operator. The map must include considerations such as:

- Circuit topology. Which magnets are connected to which controllers; series connections, shunts and boosters must be taken into account.
- Field/current calibrations of the magnet elements. Field/current curves have been estimated for each circuit from the magnet calibration data. Note that unavoidable error is introduced here if several magnets are on one circuit (with one controller). Effective lengths and apertures of the magnets are also required by the map.
- Electromagnetic hysteresis. Hysteresis effects are avoided by executing a standardizing “deGauss” cycle for all controllable elements before injection, and by keeping the ramp monotonic (i.e., no overshoot). Under these conditions the map follows the lower paths of the field/current curves, when going to a higher current.

- Strength fudges. These are empirically determined corrections to strengths as calculated by lattice design programs.
- ADC transducer calibrations. This calibration must be done so that all control readbacks can be equivalenced relative to each other.
- DAC to ADC calibrations. This calibration insures that each individual control setpoint can be equivalenced to its corresponding readback.

Our model assumes only one dipole controller. All dipole magnets are connected to this circuit in series. Successful ramping only requires that each dipole/focusing controller value be consistent relative to the others. Hence one controller ramp function is arbitrary, and the others must match it. Our model selects the dipole controller to be a straight linear DAC ramp from the initial to the final energy. That is, for a ramp of N steps:

$$\text{DAC}_{dipole}[0] = \Phi(E[0], \mathbf{S}); \quad \text{the initial dipole controller setting} \quad (2)$$

$$\text{DAC}_{dipole}[N] = \Phi(E[N], \mathbf{S}); \quad \text{the final dipole controller setting} \quad (3)$$

$$\text{DAC}_{dipole}[t] = \text{DAC}_{dipole}[0] + t * \Delta\text{DAC}_{dipole}; \quad t = 0, 1, \dots, N \quad (4)$$

where,

$$\Delta\text{DAC}_{dipole} = (\text{DAC}_{dipole}[N] - \text{DAC}_{dipole}[0])/N \quad (5)$$

At any step t , the focusing controllers must match the actual energy produced by the integer $\text{DAC}_{dipole}[t]$. If the dipole circuit had an instantaneous response, this actual energy would simply be the applied energy $\Phi^{-1}(\text{DAC}_{dipole}[t])$.

3. THE “ACTUAL” RAMP MODEL

In a real system the actual energy is not the same as the applied energy during a ramp even if the DAC values are simultaneously loaded into the controllers (within

microseconds). Nonzero response times in the control circuits and in the individual magnets will cause deviations from the ideal map Φ , particularly at the start and at the end of the ramp. This becomes more severe as operation parameters N and Δt are adjusted to get faster ramps. In our model, the combined nonzero response times of the dipole electrical circuit and of the domains in the dipole magnets are lumped into a single response time $\tau_{dipole} > 0$. Then at each step t , the actual energy change differs from the applied energy change by a constant factor:

$$\Delta E_{actual}[t] = \Delta E_{applied}[t] * \mathcal{F}_{dipole} \quad (6)$$

where,

$$\mathcal{F}_{dipole} = (1 - e^{-(\Delta t/\tau_{dipole})}) \quad (7)$$

From the increments of equation (6), the actual energy, $E_{actual}[t]$, can be accumulated for each step t . Now, the focusing strengths required to match this are:

$$\mathbf{S}[t] = d\mathbf{S}/dE * (E_{actual}[t] - E[0]) + \mathbf{S}[0] \quad (8)$$

where the vector $d\mathbf{S}/dE$ is a constant defined by:

$$d\mathbf{S}/dE = (\mathbf{S}_{final} - \mathbf{S}[0]) / (E_{final} - E[0]) \quad (9)$$

Note that $d\mathbf{S}/dE = 0$ for a pure energy ramp, and the focusing strengths do not change during the ramp. However, the controller integers that correspond to these focusing strengths always depend on the actual energy at step t :

$$DAC_{actual}[t] = \Phi(E_{actual}[t], \mathbf{S}[t]) \quad (10)$$

Finally, each of the focusing circuits k also has a lumped parameter to represent a nonzero response time. So each component k of the vector for the actual controller

integer increments differ from the corresponding component of the applied controller integer increments vector, by a constant factor:

$$\Delta \text{DAC}[k]_{\text{actual}}[t] = \Delta \text{DAC}[k]_{\text{applied}}[t] * \mathcal{F}[k] \quad (11)$$

where,

$$\mathcal{F}[k] = (1 - e^{-(\Delta t/\tau[k])}) \quad (12)$$

or,

$$\Delta \text{DAC}[k]_{\text{applied}}[t] = \Delta \text{DAC}[k]_{\text{actual}}[t]/\mathcal{F}[k] \quad (13)$$

From the increments of equation (13), the integers $\text{DAC}[k]_{\text{applied}}[t]$ can be accumulated for each controller k of a focusing element and for each step t . All of the integers:

0	$\text{DAC}_{\text{dipole}}[0]$	$\text{DAC}[1]_{\text{applied}}[0]$	$\text{DAC}[2]_{\text{applied}}[0]$...	$\text{DAC}[k]_{\text{applied}}[0]$...
1	$\text{DAC}_{\text{dipole}}[1]$	$\text{DAC}[1]_{\text{applied}}[1]$	$\text{DAC}[2]_{\text{applied}}[1]$...	$\text{DAC}[k]_{\text{applied}}[1]$...
2	$\text{DAC}_{\text{dipole}}[2]$	$\text{DAC}[1]_{\text{applied}}[2]$	$\text{DAC}[2]_{\text{applied}}[2]$...	$\text{DAC}[k]_{\text{applied}}[2]$...
:	:	:	:		:	
t	$\text{DAC}_{\text{dipole}}[t]$	$\text{DAC}[1]_{\text{applied}}[t]$	$\text{DAC}[2]_{\text{applied}}[t]$...	$\text{DAC}[k]_{\text{applied}}[t]$...

are computed as described and arranged in a table before the ramp begins. The ramp model asserts that each row of the table represents a consistent set of setpoints. When the ramp starts, each row is emitted to the controllers at timed intervals that are Δt milliseconds apart.

Note that step N usually is not the last step of the ramp, even though all of the dipole steps have been implemented. The ramp continues until all of the setpoints for each focusing controller have been implemented. This occurs when E_{actual} finally catches up and becomes essentially equal to E_{applied} (which is E_{final}).

4. ESTIMATION OF THE MODEL PARAMETERS

The ramp mapping equations have parameters, such as the response times $\tau[k]$, that must be determined empirically. This determination is done by performing repeated ramps during a “ring physics” experiment. For a pure energy ramp, the tune constants $nux[t]$ and $nuy[t]$ should not change at any time during the ramp. The tunes are observed and recorded as very precise functions of time and frequency while ramping. As the time dependencies of $nux[t]$ and $nuy[t]$ are observed, parameter values such as $\tau[k]$ are systematically assigned until the tunes are constant during pure energy ramps.

To measure the tunes, a pickup is connected to an electrode of one of the storage ring’s beam position monitors. This signal, when converted to a frequency spectrum, shows resonances at the tune values and their harmonics. The performance of the ramp can then be observed by processing this signal many times during the ramp, at a rate higher than once per ramp step interval Δt . Tune transients will be displayed as “blips” near the first and last steps of the ramp as shown in figure 2. Errors in the map Φ appear as a bow or wiggle in the middle of the ramp. Failure to compensate for these effects can result in the beam blowing up, especially in vacuum chambers that have small stay clear specifications. Once the mapping equations’ parameters have been determined, they are valid for ramps, where nux and nuy would linearly move from their values corresponding to (E_0, \mathbf{S}_0) to those for (E_{final}, S_{final}) . However, the parameters may be different for other values of the step interval Δt .

5. MEASUREMENT EQUIPMENT

Measuring the tune values requires equipment with good frequency resolution (1 kHz or less) and good time resolution (100 milliseconds or less), wide bandwidth (100’s of kHz or more), and a enough memory to capture several minutes of frequency spectra for ramp display. Most off-the-shelf test equipment is inadequate to properly measure the tunes during an energy ramp. Analog spectrum analyzers and digitizing oscilloscopes have been tried at SPEAR with little success.

An analog spectrum analyzer measures the frequency of signals by down converting the input signal into an intermediate frequency where it is measured by a resolution filter. It can also be visualized as a band pass filter “sweeping” through the frequencies of the signal. Such devices fail to observe the tune’s transient behavior, because the sweep time is usually large compared to the ramp step interval Δt .

A digitizing oscilloscope might be used to measure the tunes. However, “the wide bandwidth given by the [beam’s] short bunches requires very high sampling rates and the fast growth rates imply fast data rates. Fast data acquisition systems or digital oscilloscopes with sampling rates of many Giga samples per second have restricted triggering speeds and are usually limited in data storage.”⁴ In general, a digitizing oscilloscope that is setup to sample fast in order to capture tune transients has insufficient memory to capture an entire ramp. If the oscilloscope is set up to conserve memory, the sample rate is so slow that samples of the tunes will exhibit aliasing.

With modern DSP hardware, a parallel, filter bank analyzer has been implemented to cover wide bandwidths with narrow frequency resolution and good time resolution. A digital, parallel, filter-bank analyzer is similar to a spectrum analyzer in that it measures a signal’s frequency content or spectrum. However, “the digital filter bank analyzes an entire span of frequencies simultaneously, rather than by sweeping, and thus has an inherent speed advantage. Its frequency span is divided into side-by-side, stationary resolution bands that are slightly overlapped. The filter bank acquires signal data in a relatively short span of time and performs parallel computation of signal amplitudes in all of its resolution bands from that data. In this regard, the filter bank is similar to a conventional FFT analyzer, of which it is an outgrowth.”⁵ In addition, the output from a parallel, filter-bank can be captured in memory for spectral analysis of long periods of time. Because it exhibits a long memory length, narrow frequency resolution, short time resolution, and wide analysis bandwidth, the digital, parallel, filter-bank analyzer is an ideal instrument for measuring the tunes online during an energy ramp.

The Tektronix 3052 DSP System is an implementation of the digital, parallel, filter-bank analyzer described above, tunable from 0 to 10 MHz. The filter bank is implemented using DSP hardware on VMEbus boards. These boards process spectrums and pass data to a microcomputer on the VMEbus. The VMEbus has been modified in a fashion allowed by the VMEbus standard to create a processing "pipeline." A RAM board at the end of the processing pipeline is large enough to hold 500 frequency spectrums.

The 3052 is being used at SPEAR to observe tunes during energy ramps. In addition to fast spectral processing, the 3052 has several data display modes. First of all, it can display the spectral data in a traditional spectrum analyzer amplitude vs. frequency display. The 3052 can also display phase vs. frequency, an amplitude vs frequency waterfall, and finally a "Color Spectrogram" (see figure 2). The Color Spectrogram is most useful for observations of tunes. It is a three dimensional time versus frequency versus power plot that uses color as a third axis. The X-axis depicts frequency, the Y-axis time, and log power is represented by multicolor scaling. The time axis scrolls continuously upwards as information enters from the bottom of the display. In addition, software was written on the 3052 to display the tune fractions on the screen while the digital, parallel filter-bank is processing spectrums.

6. REFINEMENTS AND EXTENSIONS

At SPEAR, all strengths save one have independently controlled supplies. One quadrupole string has a booster supply that modifies current supplied by the dipole circuit. It was found that an additional parameter may be needed to model the combined electrical response of this circuit.

Given enough ring physics experiment time, longer ramps could be developed that would avoid possible tune resonances. These would use nonconstant strength ramp functions dS/dE so that $(nux[t], nuy[t])$ follows a prescribed path to avoid resonance points in "tune" space. Another application would be to "top off" stored beams. However, since this involves a ramp down, then a ramp up after the fill, repeated hysteresis effects would have to be taken into account in the ramp model.

CONCLUSION

The model described in this paper can be used to develop a ramping process in a storage ring. Values for some of the model parameters can be obtained by online experiments if tunes can be measured with precision, and with frequency greater than the ramp stepping rate.

ACKNOWLEDGEMENT

The authors would like to thank Martin Donald of SLAC for his help on the equations of section 3.

REFERENCES

1. A. Boyarski et al., "Automatic Control Program for SPEAR," *IEEE Transactions on Nuclear Science*, NS-20, No. 3 (1973).
2. S. Howry, T. Gromme, A. King, and M. Sullenberger, "A Portable Database Driven Control System for SPEAR," SLAC-PUB-3618 (1985).
3. M. Sands, *The Physics of Electron Storage Rings: An Introduction* (1970).
4. D. Boussard, G. Lambert, R. Lauckner, T. Linnecar, and W. Wingerter, "Real-Time Fourier Analysis for the Observation of Fast e^+e^- Instabilities in the CERN SPS," *Proceedings of the Second European Particle Accelerator Conference* (1990).
5. K. Cassidy and J. Snell, "Fast, Wideband Search for Spurious Responses," *IEEE AUTOTESTCON '91 Conference Record* (1991), pp. 383-391.

FIGURE CAPTIONS

1. Energy/strengths to DAC integers mapping Φ .
2. Time vs frequency vs power display (color spectrogram) of an energy ramp.

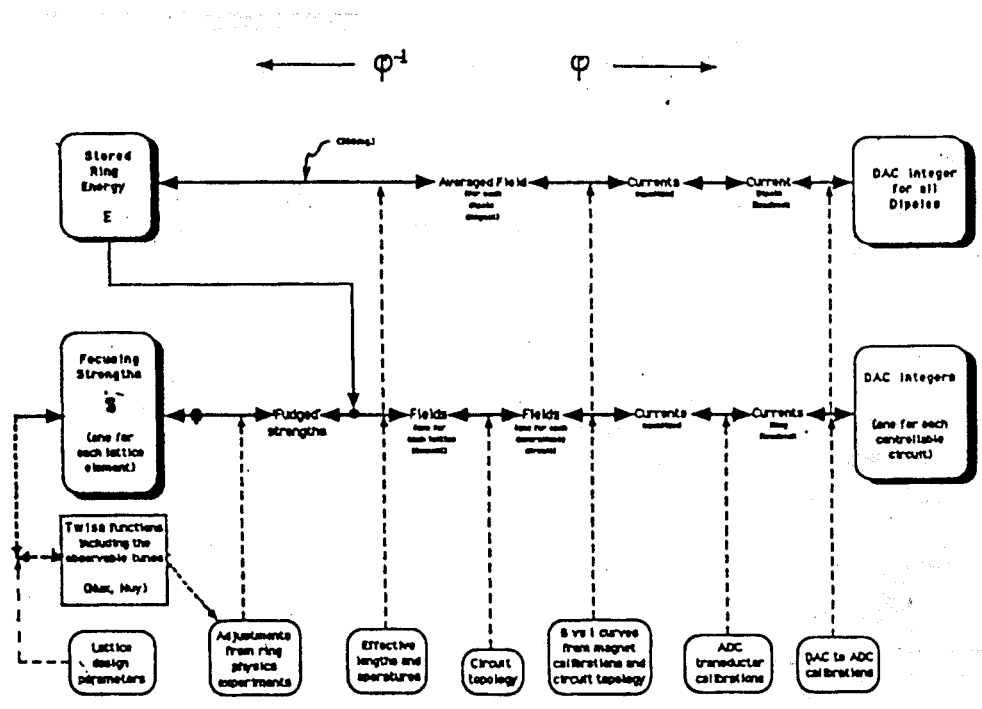


Fig. 1

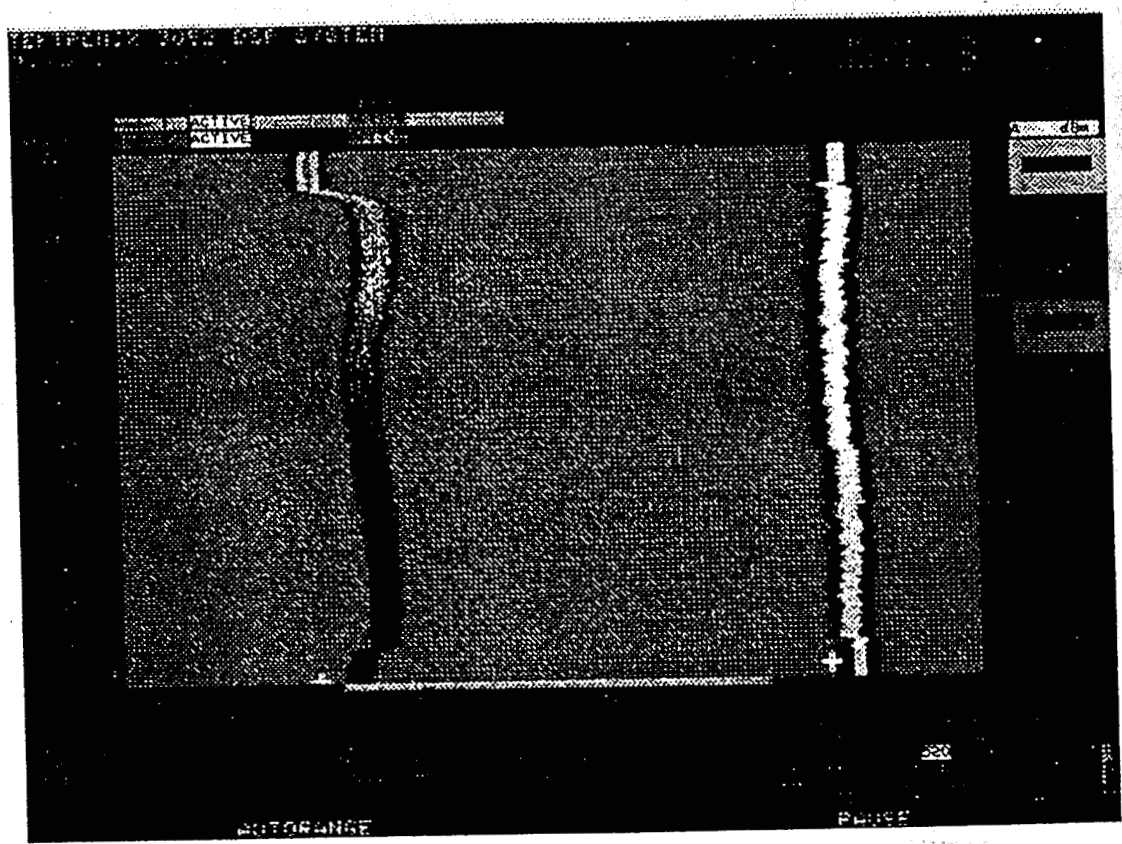


Fig. 2